Edge Distance-Based Topological Indices of Strength-Weighted Graphs and their Application to Coronoid Systems, Carbon Nanocones and SiO_2 Nanostructures

Micheal Arockiaraj[a], Sandi Klavžar[b,c,d], Joseph Clement[a],
Shagufa Mushtaq[a,*], Krishnan Balasubramanian[e]

[a]Department of Mathematics, Loyola College, Chennai 600034, India

[b]Faculty of Mathematics and Physics, University of Ljubljana, Slovenia

[c]Faculty of Natural Sciences and Mathematics, University of Maribor, Slovenia

[d]Institute of Mathematics, Physics and Mechanics, Ljubljana, Slovenia

[e]School of Molecular Sciences, Arizona State University, Tempe AZ 85287-1604, USA

Abstract

The edge-Wiener index is conceived in analogous to the traditional Wiener index and it is defined as the sum of distances between all pairs of edges of a graph G. In the recent years, it has received considerable attention for determining the variations of its computation. Motivated by the method of computation of the traditional Wiener index based on canonical metric representation, we present the techniques to compute the edge-Wiener and vertex-edge-Wiener indices of G by dissecting the original graph G into smaller strength-weighted quotient graphs with respect to Djoković-Winkler relation. These techniques have been applied to compute the exact analytic expressions for the edge-Wiener and vertex-edge-Wiener indices of coronoid systems, carbon nanocones and SiO_2 nanostructures. In addition, we have reduced these techniques to the subdivision of partial cubes and applied to the circumcoronene series of benzenoid systems.

Keywords: Canonical metric representation; Cartesian product; quotient graph; edge-Wiener index; vertex-edge-Wiener index; coronoid system.

*Corresponding author : shagufamushtaq95@gmail.com

1 Introduction

Quantitative structure-activity and structure-property relationship (QSAR/QSPR) studies have become important tools in computer aided drug discovery and predictive toxicology by providing correlations between the properties of molecules and their topology in terms of mathematical quantities. Such topological indices assist in drug discovery [5, 6] by providing efficient in-silico tools by reducing a large set of potential chemicals into smaller sets by clustering techniques on the basis of similarity of the computed topological indices. Consequently, these techniques have reduced the cost of drug discovery or simplified toxicity predictions. The significance of QSAR/QSPR study makes it crucial that appropriate descriptors are utilized to obtain proper correlations between its activities/properties and its structure. Distances between atoms and/or bonds dependences of indices such as the Wiener, the edge-Wiener, and the vertex-edge-Wiener with the best performance on the molecular structure are studied to improve their applicability for analyzing the structural activities of biomolecules by encoding the information relating to both the topology of the molecule and the chemical nature of atoms and bonds [29]. Since the activity of a molecule is closely related to its structure, graph theory has been found to be a useful tool by way of providing techniques for efficient computation of topological indices.

Chemical graph theory is an interdisciplinary science that applies graph theoretical tools to enumerate, characterize, and quantify molecular structures and spectroscopy. One of the principal areas of research in chemical graph theory is to seek techniques to reduce the topological structure of a molecule into a single number or a set of quantifiers, called the topological indices. Topological indices also aid in the synthesis of new molecules. There are various topological descriptors which are computed on the basis of topological distances, vertex degrees, hybrid degree-distances, and other connectivity based indices. The main focus of the current study are the edge-Wiener and vertex-edge-Wiener indices which are distance-based topological descriptors.

The traditional Wiener index was discovered on the basis of the observation that there exists a correlation between the boiling point of a paraffin and its molecular structures [33]. The Wiener index of a graph G is defined as the sum of topological distances between all pairs of vertices of G. It has attracted a considerable attention by many researchers in chemical and mathematical literature [28]. The edge-Wiener index was introduced in analogous to the Wiener index as the sum of the distances between all pairs of edges of G. The edge distance can in turn be defined in a couple of different ways. For two edges one can say that the distance between the edges is the minimum

distance among the end vertices of the edges, cf. [15,20]. On the other hand, it is also reasonable to consider the distance between two edges to be the distance between the corresponding vertices in the line graph, cf. [10,15]. Luckily, these two definitions differ only by the additive factor $\binom{|E(G)|}{2}$. Even before the edge-Wiener index was introduced as a topological index, it was studied in [12,13] as the Wiener index of a line graph.

In the recent years, mathematical techniques for the computation of the edge-Wiener index have been considered by a number of researchers, see [4,7,9,19,26,27,30,35,37] and a survey [14]. Motivated by the vertex and edge versions of the Wiener indices, the vertex-edge-Wiener index was introduced in [20] and it is defined as the sum of distances between all pairs of G consisting of a vertex and an edge. The standard cut method technique for the vertex-edge-Wiener index has been developed in [1,19]. The origin of the cut method, however, is the paper [23] in which the standard cut method was developed for the Wiener index. The cut method and its extensions/modifications up to the year 2015 are surveyed in [25].

It was noticed that the standard cut method based on Θ-partitions fails to characterize the topological properties of chemical structures such as coronoids and carbon nanocones. To overcome such challenges, the Θ^*-partition was efficiently used in which strength-weighted graph makes the computation elegant [2] by properly defining topological indices for strength-weighted graphs. In the graph representation of organic compounds, the atomic mass, bond lengths or bond angles, are not taken into account, where as the chemical bonding of atoms is regarded as being their most important characteristics. To measure the chemical similarity and diversity of compounds for the study of structure property relationships, topological indices such as the edge-Wiener and the vertex-edge-Wiener can be developed with a more general approach for molecular graphs containing heteroatoms and multiple bonds with strength-weighted schemes based on atomic number, covalent radius, covalent bond weights, electronegativity [16,17]. Such graphs with corresponding chemical databases can be considered as strength-weighted graphs for the efficient computation of indices compared to conventional method. The primary motivation behind working on the edge-Wiener and the vertex-edge Wiener indices is that they could be useful in determining biological activities of the molecule such as DNA binding affinity, bond path, and so on, to be deployed in the discovery of anticancer and antitumor drugs [31,36].

In this paper, we develop a method for the computation of the edge-Wiener index and the vertex-edge Wiener index of a graph G by dissecting it into quotient graphs with respect to the canonical isometric embedding of G. The principle method involves the decomposition of a graph

G into its convex components using the cut method [21, 23] by means of the transitive closure of the Djoković-Winkler relation [11, 34]. The rest of the paper is organized as follows. In Section 2, we define the graph theoretical preliminaries considered in the present study. Section 3 outlines the computational techniques and the proofs for the edge-Wiener index and the vertex-edge-Wiener index of strength-weighted graphs. In Section 4, we apply the developed techniques to compute the exact analytical expressions of the edge-Wiener index and vertex-edge-Wiener index for the coronoid systems, carbon nanocones and SiO_2 nanostructures. Furthermore, we formulate the indices discussed in the current study for the subdivision of partial cubes and apply this technique on the subdivision of circumcoronene series in Section 5. We close with concluding remarks in Section 6.

2 Graph theoretical concepts

Throughout the paper we denote a finite simple connected graph as $G = (V(G), E(G))$. The distance $d_G(u, v)$ between vertices $u, v \in V(G)$ is the lenght of a shortest u, v-path. If $e = ab \in E(G)$ and $u \in V(G)$, then the distance $d_G(u, e)$ between them is defined as $\min\{d_G(u, a), d_G(u, b)\}$. The distance $D_G(e, f)$ between edges $e = ab$ and $f = uv$ is the minimum number of edges along a shortest e, u-path or a shortest e, v-path [15, 20]. The edge-Wiener index W_e and the vertex-edge-Wiener index W_{ve} of a graph G are defined as

$$W_e(G) = \sum_{\{e,f\}\subseteq E(G)} D_G(e, f),$$

and

$$W_{ve}(G) = \sum_{u\in V(G)} \sum_{f\in E(G)} d_G(u, f).$$

The Cartesian product $G_1 \Box \cdots \Box G_k$ of graphs $G_1, \ldots, G_k$ has the vertex set $V(G_1) \times \cdots \times V(G_k)$, vertices $(u_1, \ldots, u_k)$ and $(v_1, \ldots, v_k)$ being adjacent if they differ in exactly one position, say position i, and in this position we have $u_i v_i \in E(G_i)$. The Cartesian product of graphs gives rise to important classes of graphs, for example, the n-dimensional grid is the n-fold Cartesian product of paths, while Cartesian products of complete graphs are known as Hamming graphs. In particular, the n-dimensional hypercube Q_n is the n-fold Cartesian product of K_2. Equivalently, $V(Q_n) = \{0, 1\}^n$, vertices in Q_n being adjacent if then differ in precisely one position alias bit.

A subgraph H of a graph G is said to be isometric if for any $u, v \in V(H)$, $d_H(u, v) = d_G(u, v)$. A

mapping $f : V(H) \to V(G)$ is an isometric embedding of H into G if $f(H)$ is an isometric subgraph of G. If for some n a graph H admits an isometric embedding into Q_n, then we say that H is a partial cube.

We now define the Djoković-Winkler relation Θ [11,34] which plays a crucial role in our computations. If $e = ab \in E(G)$ and $f = cd \in E(G)$, then $e\Theta f$ if $d_G(a,c) + d_G(b,d) \neq d_G(a,d) + d_G(b,c)$. The relation Θ is reflexive and symmetric, but not transitive in general. If G is a partial cube, then Θ is also transitive and hence an equivalence relation. Moereover, in that case for any Θ-class F, the graph $G - F$ consists of exactly two connected components [23]. In general, the transitive closure Θ^* of Θ forms an equivalence relation on any connected graph G and thus partitions $E(G)$ into Θ^*-classes $\mathcal{F}(G)$. If $\mathcal{F}(G) = \{F_1, \ldots, F_r\}$, then each graph $G - F_i$ consists of at least two connected components $C_1^i, \ldots, C_{r_i}^i$. The quotient graph G/F_i with respect to the part F_i of the partition $\mathcal{F}(G)$ is the graph with the vertex set $V(G/F_i) = \{C_j^i; 1 \leq j \leq r_i\}$ and the edge set $E(G/F_i) = \{C_j^i C_k^i;\ \exists\ x \in V(C_j^i)$ and $y \in V(C_k^i)$ such that $xy \in F_i\}$. Finally, a partition $\mathcal{E}(G) = \{E_1, \ldots, E_k\}$ of $E(G)$ is coarser than the partition $\mathcal{F}(G)$, if each part E_i is the union of one or more Θ^*-classes of G.

3 W_e and W_{ve} of strength-weighted graphs

The concept of a strength-weighted graph was introduced in [2] as a triple $G_{sw} = (G, SW_V, SW_E)$ where G is a simple graph and SW_V, SW_E are respectively pairs of weighted functions defined on $V(G)$ and $E(G)$:

- $SW_V = (w_v, s_v)$, where $w_v, s_v : V(G_{sw}) \to \mathbb{R}_0^+$,
- $SW_E = (w_e, s_e)$, where $w_e, s_e : E(G_{sw}) \to \mathbb{R}_0^+$.

In the context of topological indices, we restrict to the case $w_e = 1$ for every edge $e \in G_{sw}$, and henceforth $G_{sw} = (G, (w_v, s_v), s_e)$. Consequently, if $u, v \in V(G_{sw})$ and $e, f \in E(G_{sw})$, then $d_G(u,v) = d_{G_{sw}}(u,v)$, $d_G(u,f) = d_{G_{sw}}(u,f)$ and $D_G(e,f) = D_{G_{sw}}(e,f)$. The quotient graph of G_{sw} with respect to the Θ^*-class E_i of G_{sw} is defined as $G_{sw}/E_i = (G/E_i, (w_v^i, s_v^i), s_e^i)$ where the weighted functions w_v^i, s_v^i, and s_e^i are defined as follows:

- $w_v^i : V(G_{sw}/E_i) \to \mathbb{R}^+$, $w_v^i(C) = \sum\limits_{x \in V(C)} w_v(x)$, $\forall\ C \in V(G_{sw}/E_i)$,
- $s_v^i : V(G_{sw}/E_i) \to \mathbb{R}^+$, $s_v^i(C) = \sum\limits_{xy \in E(C)} s_e(xy) \ + \sum\limits_{x \in V(C)} s_v(x)$, $\forall\ C \in V(G_{sw}/E_i)$,

- $s_e^i : E(G_{sw}/E_i) \to \mathbb{R}^+$, $s_e^i(CD) = \sum_{\substack{xy \in E_i \\ x \in V(C),\ y \in V(D)}} s_e(xy), \forall\ CD \in E(G_{sw}/E_i)$.

The vertex distance-based, degree-distance-based and counting related topological indices have already been defined for strength-weighted graph in [2]. Moreover, if $w_v = s_e \equiv 1$ and $s_v \equiv 0$ for a topological index TI, then $TI(G_{sw}) = TI(G)$. In this way, we now carefully define the edge distance-based topological indices such as the edge-Wiener index and the vertex-edge-Wiener index for strength-weighted graphs in order to devise an elegant general method for their computation of indices.

Definition 1. *The edge-Wiener index of a strength-weighted graph G_{sw} is*

$$W_e(G_{sw}) = \sum_{\{u,v\} \subseteq V(G_{sw})} s_v(u)\ s_v(v)\ d_{G_{sw}}(u,v) + \sum_{\{e,f\} \subseteq E(G_{sw})} s_e(e)\ s_e(f)\ D_{G_{sw}}(e,f) + \sum_{u \in V(G_{sw})} \sum_{f \in E(G_{sw})} s_v(u)\ s_e(f)\ d_{G_{sw}}(u,f). \tag{1}$$

Definition 2. *The vertex-edge-Wiener index of a strength-weighted graph G_{sw} is*

$$W_{ve}(G_{sw}) = \sum_{\{u,v\} \subseteq V(G_{sw})} \left\{ w_v(u)\ s_v(v) + w_v(v)\ s_v(u) \right\} d_{G_{sw}}(u,v) + \sum_{u \in V(G_{sw})} \sum_{f \in E(G_{sw})} w_v(u)\ s_e(f)\ d_{G_{sw}}(u,f). \tag{2}$$

Prior to strength-weighted graphs, there were techniques for computing the vertex distance-based topological indices by considering the vertex-weights [8, 22, 24] and following these ideas and extending some of the insights of benzenoid systems [9, 19], a technique, based on the seminal paper in this direction [19], was recently developed [32] for the edge-Wiener index by considering edge-weights. Actually, the technique was converting the problem of computing the edge-Wiener index to the problem of computing the sum of the Wiener index, edge-Wiener index and vertex-edge-Wiener index of weighted quotient graphs corresponding to the Θ^*-classes, in parallel to the approach from [19] for Θ-classes. What we now notice is that graphs under question are edge-weighted graphs and that the technique converts graphs into both vertex and edge-weighted graphs, which implies that the technique is not iterative in nature. Since the notations are somehow inconsistent when one intends to find both vertex and edge distance-based topological indices, we believe that the strength-weighted graphs will be useful for this purpose with any combination of vertex and edge-weighted functions. For the sake of completeness, we prove the following theorem and, in

addition, extend the idea to the vertex-edge-Wiener index.

Theorem 3. *Let $G_{sw} = \big(G, (w_v, s_v), s_e\big)$ be a strength-weighted graph and $\mathcal{E}(G_{sw}) = \{E_1, \ldots, E_k\}$ a partition of $E(G)$ coarser than $\mathcal{F}'(G_{sw})$. If $TI \in \{W_e, W_{ve}\}$, then*

$$TI(G_{sw}) = \sum_{i=1}^{k} TI(G/E_i, (w_v^i, s_v^i), s_e^i).$$

Proof. Since $V(G_{sw}) = V(G)$, $E(G_{sw}) = E(G)$, $d_{G_{sw}} = d_G$, and $D_{G_{sw}} = D_G$, we can follow the contraction mappings of canonical metric representations from [21, 32]. Let $\ell_i : V(G) \to V(G/E_i)$ be given by $\ell_i(x) = C_j^i$, where C_j^i is the connected component of $G - E_i$ such that $x \in C_j^i$. Define now the mapping $\alpha_i : E(G) \to V(G/E_i) \cup E(G/E_i)$ as

$$\alpha_i(xy) = \begin{cases} \ell_i(x) \in V(G/E_i); & \{x, y\} \subseteq V(C_j^i), \\ \ell_i(x)\ell_i(y) \in E(G/E_i); & x \in V(C_j^i), y \in V(C_k^i). \end{cases}$$

Furthermore, it was already proved that the distance between two vertices [24] and distance between two edges [32] can be computed by using the distances in the quotient graphs as follows:

$$\begin{aligned} d_G(u, v) &= \sum_{i=1}^{k} d_{G/E_i}(\ell_i(u), \ell_i(v)), \\ D_G(e, f) &= \sum_{i=1}^{k} D_{G/E_i}(\alpha_i(e), \alpha_i(f)). \end{aligned}$$

In a similar way, one can prove that the distance between vertex and edge can be obtained by using the distances in the quotient graph as follows:

$$d_G(u, f) = \sum_{i=1}^{k} d_{G/E_i}(\ell_i(u), \alpha_i(f)).$$

Using these facts we complete the proof in the following two cases.

Case 1: $(TI = W_e)$

$$\begin{aligned} W_e(G_{sw}) = &\sum_{\{u,v\} \subseteq V(G)} s_v(u)\ s_v(v)\ d_{G_{sw}}(u, v) + \sum_{\{e,f\} \subseteq E(G)} s_e(e)\ s_e(f)\ D_{G_{sw}}(e, f) \\ &+ \sum_{u \in V(G)} \sum_{f \in E(G)} s_v(u)\ s_e(f)\ d_{G_{sw}}(u, f) \end{aligned}$$

$$
\begin{aligned}
&= \sum_{\{u,v\}\subseteq V(G)} s_v(u)\ s_v(v)\ \Big(\sum_{i=1}^{k} d_{G/E_i}(\ell_i(u),\ell_i(v))\Big) \\
&\quad + \sum_{\{e,f\}\subseteq E(G)} s_e(e)\ s_e(f)\ \Big(\sum_{i=1}^{k} D_{G/E_i}(\alpha_i(e),\alpha_i(f))\Big) \\
&\quad + \sum_{u\in V(G)}\sum_{f\in E(G)} s_v(u)\ s_e(f)\ \Big(\sum_{i=1}^{k} d_{G/E_i}(\ell_i(u),\alpha_i(f))\Big) \\
&= \sum_{i=1}^{k}\Big(\sum_{\{\ell_i(u),\ell_i(v)\}\subseteq V(G/E_i)} s_v^i(\ell_i(u))\ s_v^i(\ell_i(v))\ d_{G/E_i}\big(\ell_i(u),\ell_i(v)\big) \\
&\qquad + \sum_{\{\alpha_i(e),\alpha_i(f)\}\subseteq E(G/E_i)} s_e^i(\alpha_i(e))\ s_e^i(\alpha_i(f))\ D_{G/E_i}\big(\alpha_i(e),\alpha_i(f)\big) \\
&\qquad + \sum_{\ell_i(u)\in V(G/E_i)}\sum_{\alpha_i(f)\in E(G/E_i)} s_v^i(\ell_i(u))\ s_e^i(\alpha_i(f))\ d_{G/E_i}\big(\ell_i(u),\alpha_i(f)\big)\Big) \\
&= \sum_{i=1}^{k} W_e(G/E_i,(w_v^i,s_v^i),s_e^i).
\end{aligned}
$$

Case 2: $(TI = W_{ve})$

$$
\begin{aligned}
W_{ve}(G_{sw}) &= \sum_{\{u,v\}\subseteq V(G_{sw})} \Big[w_v(u)\ s_v(v)\ +\ w_v(v)\ s_v(u)\Big]\ d_{G_{sw}}(u,v) \\
&\quad + \sum_{u\in V(G_{sw})}\sum_{f\in E(G_{sw})} w_v(u)\ s_e(f)\ d_{G_{sw}}(u,f) \\
&= \sum_{\{u,v\}\subseteq V(G)} \Big[w_v(u)\ s_v(v)\ +\ w_v(v)\ s_v(u)\Big]\ \Big(\sum_{i=1}^{k} d_{G/E_i}(\ell_i(u),\ell_i(v))\Big) \\
&\quad + \sum_{u\in V(G)}\sum_{f\in E(G)} w_v(u)\ s_e(f)\ \Big(\sum_{i=1}^{k} d_{G/E_i}(\ell_i(u),\alpha_i(f))\Big) \\
&= \sum_{i=1}^{k}\Big(\sum_{\{\ell_i(u),\ell_i(v)\}\subseteq V(G/E_i)} \Big[w_v^i(\ell_i(u))\ s_v^i(\ell_i(v))\ + w_v^i(\ell_i(v))\ s_v^i(\ell_i(u))\Big] \\
&\qquad\qquad d_{G/E_i}\big(\ell_i(u),\ell_i(v)\big) \\
&\qquad + \sum_{\ell_i(u)\in V(G/E_i)}\sum_{\alpha_i(f)\in E(G/E_i)} w_v^i(\ell_i(u))\ s_e^i(\alpha_i(f))\ d_{G/E_i}\big(\ell_i(u),\alpha_i(f)\big)\Big) \\
&= \sum_{i=1}^{k} W_{ve}(G/E_i,(w_v^i,s_v^i),s_e^i).
\end{aligned}
$$

□

We now exemplify the technique for obtaining the expressions of the edge-Wiener index and the vertex-edge-Wiener index of strength-weighted graphs. Consider the graph G as depicted in Figure 1(a). The Θ^*-classes E_1 and E_2 of G are shown in Figures 1(b) and 1(c), respectively. The strength-weighted graphs of G with respect to the Θ^*-classes are given in Figures 2(a) and 2(b).

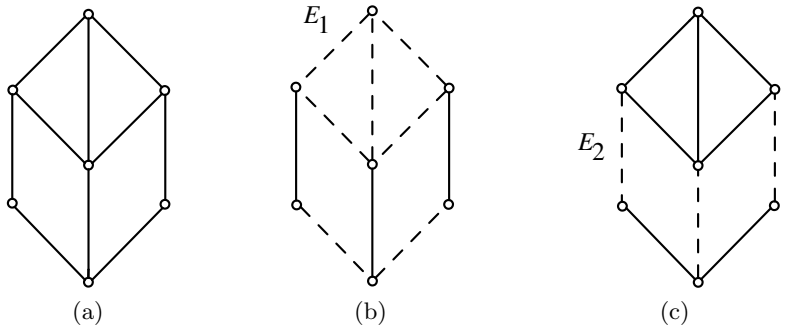

Figure 1: A graph G with Θ^*-classes.

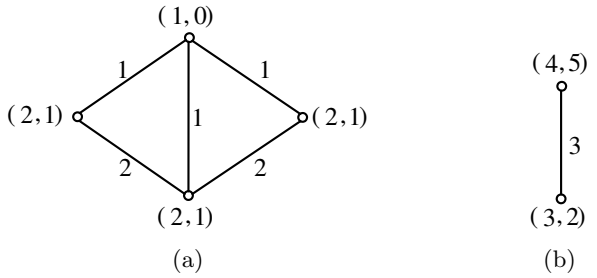

Figure 2: Strength-weighted quotient graphs (a) G/E_1 (b) G/E_2.

We now calculate the edge-Wiener index of the two quotient graphs individually by using Eqn. (1) and then sum them up to obtain the edge-Wiener index of G, that is,

$$W_e(G) = W_e(G/E_1, (w_v^1, s_v^1), s_e^1) + W_e(G/E_2, (w_v^2, s_v^2), s_e^2).$$

In view of (1) we set $W_e(G/E_i) = W_e^1(G/E_i) + W_e^2(G/E_i) + W_e^3(G/E_i)$, where

$$\begin{aligned}
W_e^1(G/E_i) &= \sum_{\{u,v\}\subseteq V(G/E_i)} s_v(u)\ s_v(v)\ d_{G_{sw}}(u,v),\\
W_e^2(G/E_i) &= \sum_{\{e,f\}\subseteq E(G/E_i)} s_e(e)\ s_e(f)\ D_{G_{sw}}(e,f),\\
W_e^3(G/E_i) &= \sum_{u\in V(G/E_i)} \sum_{f\in E(G/E_i)} s_v(u)\ s_e(f)\ d_{G_{sw}}(u,f).
\end{aligned}$$

For the quotient graph G/E_1, the edge-Wiener index is computed as follows:

$$W_e^1(G/E_1) = 1 \cdot 1(1) + 1 \cdot 1(2) + 1 \cdot 1(1) = 4,$$
$$W_e^2(G/E_1) = 1 \cdot 2(1) + 2 \cdot 1(1) = 4,$$
$$W_e^3(G/E_1) = 1 \cdot 1(1) + 1 \cdot 2(1) + 1 \cdot 1(1) + 1 \cdot 1(1) + 1 \cdot 1(1) + 1 \cdot 1(1) + 1 \cdot 2(1) + 1 \cdot 1(1) = 10.$$

We conclude that $W_e(G/E_1) = 4 + 4 + 10 = 18$.

Similarly, we compute for the quotient graph G/E_2: $W_e^1(G/E_2) = 5 \cdot 2(1) = 10$, $W_e^2(G/E_2) = 0$, $W_e^3(G/E_2) = 0$. Hence $W_e(G/E_2) = 10$ and thus

$$W_e(G) = W_e(G/E_1) + W_e(G/E_2) = 28.$$

We next proceed to compute the vertex-edge-Wiener index for the graph G from Figure 1 by following the same technique, where we have

$$W_{ve}(G) = W_{ve}(G/E_1, (w_v^1, s_v^1), s_e^1) + W_{ve}(G/E_2, (w_v^2, s_v^2), s_e^2).$$

Again in view of (2) we set $W_{ve}(G/E_i) = W_{ve}^1(G/E_i) + W_{ve}^2(G/E_i)$, where

$$W_{ve}^1(G/E_i) = \sum_{\{u,v\} \subseteq V(G/E_i)} \{w_v(u)\ s_v(v) + w_v(v)\ s_v(u)\}\ d_{G_{sw}}(u, v),$$
$$W_{ve}^2(G/E_i) = \sum_{u \in V(G/E_i)} \sum_{f \in E(G/E_i)} w_v(u)\ s_e(f)\ d_{G_{sw}}(u, f).$$

Then,

$$W_{ve}^1(G/E_1) = 1 \cdot 1 + 2 \cdot 1 + 1 \cdot 2 + 2(2 \cdot 1 + 1 \cdot 2) + 1 \cdot 1 + 1 \cdot 1 + 2 \cdot 1 + 1 \cdot 2 = 19,$$
$$W_{ve}^2(G/E_1) = 2 \cdot 1 + 2 \cdot 2 + 1 \cdot 2 + 1 \cdot 2 + 2 \cdot 1 + 2 \cdot 2 + 2 \cdot 1 + 2 \cdot 1 + 2 \cdot 1 + 2 \cdot 1 = 24,$$
$$W_{ve}(G/E_1) = 19 + 24 = 43.$$

Similarly, $W_{ve}^1(G/E_2) = 4 \cdot 2 + 5 \cdot 3 = 23$, $W_{ve}^2(G/E_2) = 0$, $W_{ve}(G/E_2) = 23$, and therefore,

$$W_{ve}(G) = W_{ve}(G/E_1) + W_{ve}(G/E_2) = 43 + 23 = 66.$$

4 Computation of W_e and W_{ve} for certain molecular structures

In this section, we apply the formulas obtained in Theorem 3 to compute the edge-Wiener index and the vertex-edge-Wiener index of coronoid systems, carbon nanocones, and SiO_2 nanostructures.

4.1 Coronoid systems

A benzenoid system is a finite connected substructure of the parent infinite hexagonal system which is obtained by arranging regular hexagons with no cut vertices such that two hexagons are either disjoint or have a common edge between them. A coronoid system is obtained from a benzenoid system by deleting few interior vertices and their corresponding edges to form a unique interior face bounded by a polygon of length greater than six.

The circumcision process of obtaining structures with polygonal holes pose considerable challenges in computing indices of such structures. In [2], the authors have computed various distance-based, degree-distance-based and counting related topological indices by applying the concept of strength-weighted graphs on the coronoid structures. To proceed with the computation of the edge-Wiener index of such coronoid systems, we refer to [2] for the cuts and the strength-weighted values of the quotient graphs.

Theorem 4. *Let G be the $K_1(n,p,q,r)$ coronoid structure, where $r \geq 1$, $n \geq 3$, and $1 \leq p = q \leq n$. Then,*

1. $W_e(G) = \frac{1}{2}(36n^3r^2+216n^2pr^2+126n^2r^3+432np^2r^2+504npr^3+189nr^4+288p^3r^2+504p^2r^3+378pr^4+144r^5+48n^3r+288n^2pr-138n^2r^2+576np^2r-528npr^2-450nr^3+384p^3r-540p^2r^2-900pr^3-339r^4+16n^3+96n^2p-350n^2r+192np^2-1392npr+21nr^2+128p^3-1396p^2r+30pr^2+388r^3-136n^2-544np+824nr-544p^2+1644pr+238r^2+384n+768p-625r-360)$.

2. $W_{ve}(G) = \frac{1}{6}(144n^3r^2+864n^2pr^2+504n^2r^3+1728np^2r^2+2016npr^3+756nr^4+1152p^3r^2+2016p^2r^3+1512pr^4+576r^5+240n^3r+1440n^2pr-312n^2r^2+2880np^2r-1200npr^2-1350nr^3+1920p^3r-1224p^2r^2-2700pr^3-975r^4+96n^3+576n^2p-1584n^2r+1152np^2-6288npr-696nr^2+768p^3-6312p^2r-1416pr^2+758r^3-768n^2-3072np+3354nr-3072p^2+6684pr+1515r^2+2040n+4080p-2210r-1800)$.

Proof. The coronoid structure $K_1(n,p,q,r)$ depicted in Figure 3 has $|V(G)| = 2(r+1)(2n+4p+3r-5)$ and $|E(G)| = 3(r+2)(2n+4p+3r-5)$. Due to the presence of the cavity, the Θ^*-classes on the structure are along the periphery of the cavity and the boundary of the cavity as shown in

Figure 3. There are $2r$ horizontal cuts on the periphery of which r horizontal cuts $\{E_{hi} : 1 \leq i \leq r\}$ along the North direction are symmetric to the r horizontal edge cuts along the South direction. Similarly, there are other $4r$ cuts along the periphery of which r acute cuts $\{E_{ai} : 1 \leq i \leq r\}$ running respectively along the North-West and South-East directions are symmetric to the r obtuse cuts respectively along the North-East and South-West directions. There are $n + 2p - 1$ middle edge cuts along the boundary of the hole in which E_2, E_3 cuts are symmetric to E_1 and the remaining $n + 2p - 4$ cuts which are symmetric to E_4 are shown in Figure 3. Hence, the total number of Θ^*-classes in G is $6r + n + 2p - 1$. Their corresponding quotient graphs along with strength-weighted functions are shown in Figure 4. The strength-weighted functions whose values are not given in the figure are presented in Table 1.

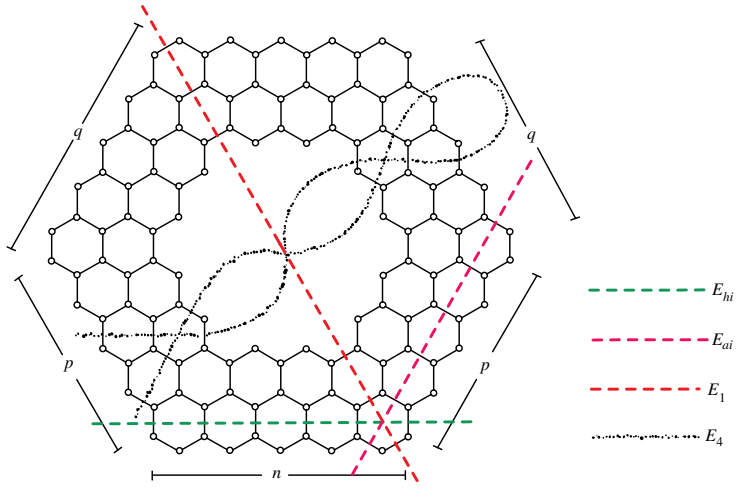

Figure 3: Coronoid structure $K_1(n, p, q, r)$ with typical Θ^*-classes.

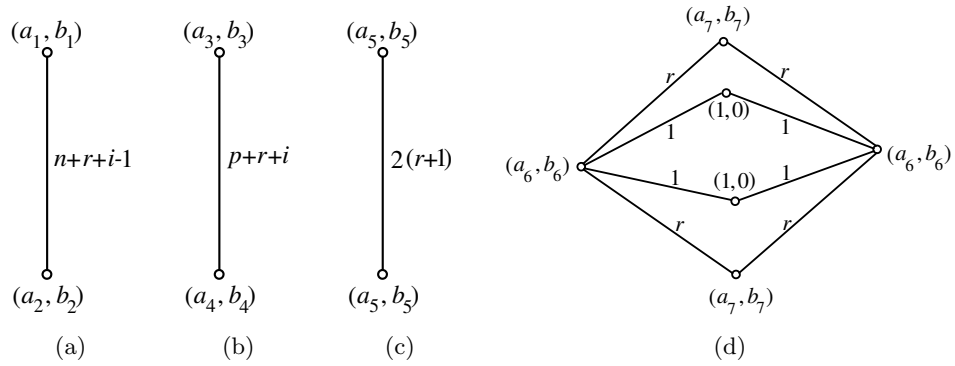

Figure 4: Quotient graphs (a) G/E_{hi} (b) G/E_{ai} (c) G/E_1 (d) G/E_4.

Table 1: Strength-weighted values for the quotient graphs of $K_1(n,p,q,r)$.

Quotient graphs	$\boldsymbol{w_v}$	$\boldsymbol{s_v}$
G/E_{hi}; $1 \le i \le r$	$a_1 = i(i+2n+2r-2)$ $a_2 = \lvert V(G)\rvert - a_1$	$b_1 = \frac{1}{2}(6in-2n-2r-9i+6ir+3i^2+2)$ $b_2 = \lvert E(G)\rvert - b_1 - (n+r+i-1)$
G/E_{ai}; $1 \le i \le r$	$a_3 = i(i+2p+2r)$ $a_4 = \lvert V(G)\rvert - a_3$	$b_3 = \frac{1}{2}(6ip-2p-2r-3i+6ir+3i^2)$ $b_4 = \lvert E(G)\rvert - b_3 - (p+r+i)$
G/E_i; $1 \le i \le 3$	$a_5 = (r+1)(2n+4p+3r-5)$	$b_5 = \frac{1}{2}(4n+8p-11r+6nr+$ $12pr+9r^2-12)$
G/E_i; $4 \le i \le n+2p-1$	$a_6 = 2(n+2p-r+nr+$ $2pr+r^2-3)$ $a_7 = r^2$	$b_6 = 2n+4p-5r+3nr+6pr+3r^2-7$ $b_7 = \frac{3}{2}r(r-1)$

We denote

$$W_e(G_1) \;=\; \sum_{i=1}^{r} W_e(G/E_{hi},(w_v^{hi},s_v^{hi}),s_e^{hi}) \;=\; \sum_{i=1}^{r} b_1 b_2,$$

$$W_e(G_2) \;=\; \sum_{i=1}^{r} W_e(G/E_{ai},(w_v^{ai},s_v^{ai}),s_e^{ai}) \;=\; \sum_{i=1}^{r} b_3 b_4,$$

$$W_e(G_3) \;= W_e(G/E_i,(w_v^{i},s_v^{i}),s_e^{i}) \;=\; b_5^2,$$

$$\begin{aligned} W_e(G_4) \;&= W_e(G/E_i,(w_v^{i},s_v^{i}),s_e^{i}) \\ &= 2\Big(2b_6b_7+b_6^2+b_7^2+r^2+4r+1+2\big(rb_6+b_6+rb_7+2b_7\big)\Big). \end{aligned}$$

Therefore,

$$W_e(G) \;= 2W_e(G_1)+4W_e(G_2)+3W_e(G_3)+(n+2p-4)W_e(G_4),$$

from which the stated expression is routinely computed.

We proceed similarly in order to obtain the vertex-edge-Wiener index. Denote,

$$W_{ve}(G_1) = \sum_{i=1}^{r} W_{ve}(G/E_{hi},(w_v^{hi},s_v^{hi}),s_e^{hi}) = \sum_{i=1}^{r} \big(a_1b_2+a_2b_1\big),$$

$$W_{ve}(G_2) = \sum_{i=1}^{r} W_{ve}(G/E_{ai}, (w_v^{ai}, s_v^{ai}), s_e^{ai}) = \sum_{i=1}^{r} \big(a_3b_4 + a_4b_3\big),$$

$$W_{ve}(G_3) = W_{ve}(G/E_i, (w_v^i, s_v^i), s_e^i) = 2a_5b_5,$$

$$\begin{aligned} W_{ve}(G_4) =& W_{ve}(G/E_i, (w_v^i, s_v^i), s_e^i) \\ =& 4\bigg(a_6b_7 + a_7b_6 + a_6b_6 + a_7b_7 + b_6 + 2b_7 + a_6 + 2a_7 + r(a_6 + a_7 + 2) + 1\bigg). \end{aligned}$$

Therefore,

$$W_{ve}(G) \ = 2W_{ve}(G_1) + 4W_{ve}(G_2) + 3W_{ve}(G_3) + (n + 2p - 4)W_{ve}(G_4),$$

from which the stated expression is obtained routinely. □

Since r-circumscribed $C_{32}H_{16}$ and $C_{48}H_{24}$ are the special cases of $K_1(n, p, q, r)$, we substitute $K(3, 1, 1, r)$ and $K(3, 2, 2, r)$ respectively into the analytical expressions obtained in Theorem 4 to compute their edge-Wiener and vertex-edge-Wiener indices.

Corollary 1. *For $r \geq 1$, let G be an r-circumscribed $C_{32}H_{16}$ coronoid structure. Then,*

1. $W_e(G) = \frac{1}{2}(144r^5 + 606r^4 + 1288r^3 + 1465r^2 + 769r + 160)$.
2. $W_{ve}(G) = \frac{1}{6}(576r^5 + 2805r^4 + 6608r^3 + 8379r^2 + 5104r + 1200)$.

Corollary 2. *For $r \geq 1$, let G be an r-circumscribed $C_{48}H_{24}$ coronoid structure. Then,*

1. $W_e(G) = \frac{1}{2}(144r^5 + 984r^4 + 3412r^3 + 6139r^2 + 4513r + 1152)$.
2. $W_{ve}(G) = \frac{1}{6}(576r^5 + 4317r^4 + 16004r^3 + 31083r^2 + 26308r + 7776)$.

Theorem 5. *Let G be the $K_2(n, p, q, r)$ coronoid structure, where $r \geq 1$, $n \geq 3$, and $1 \leq p < q \leq n$. Then*

1. $W_e(G) = \frac{1}{10}(180n^3r^2 + 540n^2pr^2 + 540n^2qr^2 + 660n^2r^3 + 540np^2r^2 + 1080npqr^2 + 1440npr^3 + 540nq^2r^2 + 1440nqr^3 + 1230nr^4 + 180p^3r^2 + 540p^2qr^2 + 660p^2r^3 + 540pq^2r^2 + 1440pqr^3 + 1230pr^4 + 180q^3r^2 + 660q^2r^3 + 1230qr^4 + 738r^5 + 240n^3r + 720n^2pr + 720n^2qr - 630n^2r^2 + 720np^2r + 1440npqr - 1140npr^2 + 720nq^2r - 1140nqr^2 - 2080nr^3 + 240p^3r + 720p^2qr - 630p^2r^2 + 720pq^2r - 1140pqr^2 - 2200pr^3 + 240q^3r - 630q^2r^2 - 2200qr^3 - 2250r^4 + 80n^3 + 240n^2p + 240n^2q - 1720n^2r +$

$240np^2+480npq-3440npr+240nq^2-3440nqr-150nr^2+80p^3+240p^2q-1720p^2r+240pq^2-3440pqr-270pr^2+80q^3-1720q^2r-270qr^2+1120r^3-680n^2-1360np-1360nq+3960nr-680p^2-1360pq+3960pr-680q^2+3960qr+1305r^2+1920n+1920p+1920q-2843r-1800)$.

2. $W_{ve}(G) = \frac{1}{15}(360n^3r^2+1080n^2pr^2+1080n^2qr^2+1320n^2r^3+1080np^2r^2+2160npqr^2+2880npr^3+1080nq^2r^2+2880nqr^3+2460nr^4+360p^3r^2+1080p^2qr^2+1320p^2r^3+1080pq^2r^2+2880pqr^3+2460pr^4+360q^3r^2+1320q^2r^3+2460qr^4+1476r^5+600n^3r+1800n^2pr+1800n^2qr-630n^2r^2+1800np^2r+3600npqr-960npr^2+1800nq^2r-960nqr^2-2680nr^3+600p^3r+1800p^2qr-630p^2r^2+1800pq^2r-960pqr^2-2920pr^3+600q^3r-630q^2r^2-2920qr^3-3480r^4+240n^3+720n^2p+720n^2q-3870n^2r+720np^2+1440npq-7680npr+720nq^2-7680nqr-2085nr^2+240p^3+720p^2q-3870p^2r+720pq^2-7680pqr-2385pr^2+240q^3-3870q^2r-2385qr^2-440r^3-1920n^2-3840np-3840nq+7975nr-1920p^2-3840pq+7915pr-1920q^2+7915qr+3195r^2+5100n+5100p+5100q-5101r-4500)$.

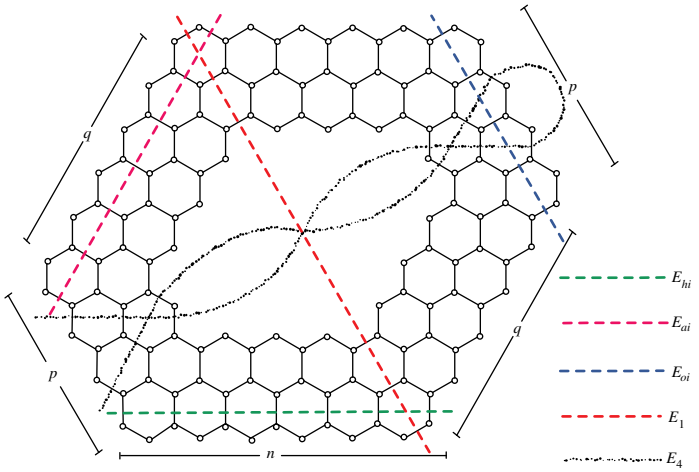

Figure 5: Coronoid structure $K_2(n,p,q,r)$ with its typical Θ^*-classes.

Proof. The coronoid structure $K_2(n,p,q,r)$ depicted in Figure 5 has $|V(G)| = 2(r+1)(2n+2p+2q+3r-5)$ and $|E(G)| = (3r+2)(2n+2p+2q+3r-5)$. Applying the Djoković-Winkler relation, the Θ^*-classes on this coronoid structure along the periphery of the cavity, there are r horizontal cuts $\{E_{hi} : 1 \leq i \leq r\}$ along the North direction which are symmetric to another r horizontal cuts along the South direction; r acute cuts $\{E_{ai} : 1 \leq i \leq r\}$ along the South-East direction symmetric to another r acute cuts along the North-West direction; and r obtuse cuts $\{E_{oi} : 1 \leq i \leq r\}$ along the South-West direction symmetric to r obtuse cuts along the North-East direction; while the Θ^*-classes along the boundary of the hole consists of $n+p+q-1$ middle cuts in which 3 cuts are

symmetric to E_1 and $n+p+q-4$ cuts are symmetric to E_4 as shown in the Figure 5. Hence, there are a total of $6r+n+p+q-1$ number of Θ^*-classes in G. The corresponding quotient graphs obtained on applying these cuts along with their strength-weighted functions are shown in Figure 6 and the vertex-strength-weighted functions not defined in the Figure 6 are shown in Table 2.

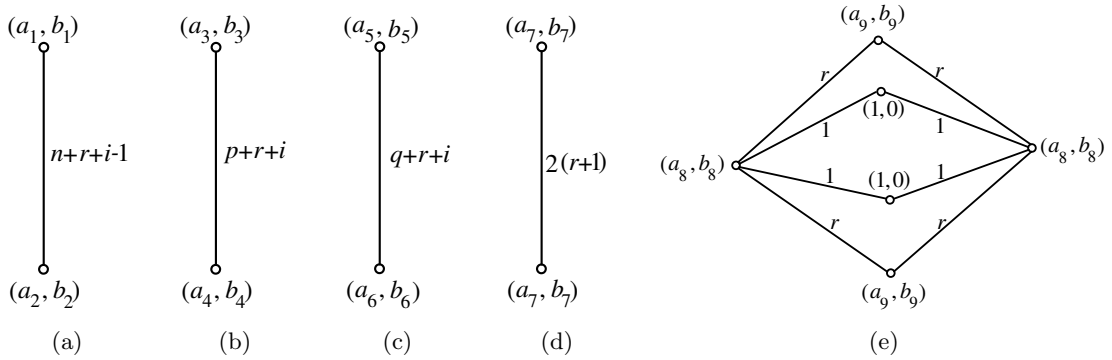

Figure 6: Quotient graphs (a) G/E_{hi} (b) G/E_{ai} (c) G/E_{oi} (d) G/E_1 (e) G/E_4.

Table 2: Strength-weighted values for the quotient graphs of $K_2(n,p,q,r)$.

Quotient graphs	$\boldsymbol{w_v}$	$\boldsymbol{s_v}$
G/E_{hi};	$a_1 = i(i+2n+2r-2)$	$b_1 = \frac{1}{2}(6in-2n-2r-9i+6ir+3i^2+2)$
$1 \le i \le r$	$a_2 = \|V(G)\| - a_1$	$b_2 = \|E(G)\| - b_1 - (n+r+i-1)$
G/E_{ai};	$a_3 = i(i+2p+2r)$	$b_3 = \frac{1}{2}(6ip-2p-2r-3i+6ir+3i^2)$
$1 \le i \le r$	$a_4 = \|V(G)\| - a_3$	$b_4 = \|E(G)\| - b_3 - (p+r+i)$
G/E_{oi};	$a_5 = i(i+2q+2r)$	$b_5 = \frac{1}{2}(6iq-2q-2r-3i+6ir+3i^2)$
$1 \le i \le r$	$a_6 = \|V(G)\| - a_5$	$b_6 = \|E(G)\| - b_5 - (q+r+i)$
G/E_i;	$a_7 = (r+1)(2n+2p+$	$b_7 = \frac{1}{2}(4n+4p+4q-11r+6nr+$
$1 \le i \le 3$	$2q+3r-5)$	$6pr+6qr+9r^2-12)$
G/E_i;	$a_8 = 2(n+p+q-r+$	$b_8 = 2n+2p+2q-5r+3nr+3pr+$
$4 \le i \le n+p+q-1$	$nr+pr+qr+r^2-3)$	$3qr+3r^2-7$
	$a_9 = r^2$	$b_9 = \frac{3}{2}r(r-1)$

We denote

$$W_e(G_1) \;=\; \sum_{i=1}^{r} W_e(G/E_{hi}, (w_v^{hi}, s_v^{hi}), s_e^{hi}) \;=\; \sum_{i=1}^{r} b_1 b_2,$$

$$W_e(G_2) \;=\; \sum_{i=1}^{r} W_e(G/E_{ai},(w_v^{ai},s_v^{ai}),s_e^{ai}) \;=\; \sum_{i=1}^{r} b_3b_4,$$

$$W_e(G_3) \;=\; \sum_{i=1}^{r} W_e(G/E_{oi},(w_v^{oi},s_v^{oi}),s_e^{oi}) \;=\; \sum_{i=1}^{r} b_5b_6,$$

$$W_e(G_4) \;= W_e(G/E_i,(w_v^{i},s_v^{i}),s_e^{i}) \;=\; b_7^2,$$

$$\begin{aligned} W_e(G_5) \;&= W_e(G/E_i,(w_v^{i},s_v^{i}),s_e^{i}) \\ &= 2\Big(2b_8b_9 + b_8^2 + b_9^2 + r^2 + 4r + 1 + 2\big(rb_8 + b_8 + rb_9 + 2b_9\big)\Big). \end{aligned}$$

Therefore,

$$W_e(G) \;= 2W_e(G_1) + 2W_e(G_2) + 2W_e(G_3) + 3W_e(G_4) + (n+p+q-4)W_e(G_5).$$

Similarly, we obtain for the vertex-edge-Wiener index as follows.

$$W_{ve}(G_1) \;=\; \sum_{i=1}^{r} W_{ve}(G/E_{hi},(w_v^{hi},s_v^{hi}),s_e^{hi}) = \sum_{i=1}^{r} \big(a_1b_2 + a_2b_1\big),$$

$$W_{ve}(G_2) \;=\; \sum_{i=1}^{r} W_{ve}(G/E_{ai},(w_v^{ai},s_v^{ai}),s_e^{ai}) = \sum_{i=1}^{r} \big(a_3b_4 + a_4b_3\big),$$

$$W_{ve}(G_3) \;=\; \sum_{i=1}^{r} W_{ve}(G/E_{oi},(w_v^{oi},s_v^{oi}),s_e^{oi}) = \sum_{i=1}^{r} \big(a_5b_6 + a_6b_5\big),$$

$$W_{ve}(G_4) \;= W_{ve}(G/E_i,(w_v^{i},s_v^{i}),s_e^{i} = 2a_7b_7,$$

$$\begin{aligned} W_{ve}(G_5) \;&= W_{ve}(G/E_i,(w_v^{i},s_v^{i}),s_e^{i}) \\ &= 4\Big(a_8b_9 + a_9b_8 + a_8b_8 + a_9b_9 + b_8 + 2b_9 + a_8 + 2a_9 + r(a_8+a_9+2) + 1\Big). \end{aligned}$$

Therefore,

$$W_{ve}(G) \;= 2W_{ve}(G_1) + 2W_{ve}(G_2) + 2W_{ve}(G_3) + 3W_{ve}(G_4) + (n+p+q-4)W_{ve}(G_5),$$

from which we obtain the expression. □

Corollary 3. *For $r \geq 1$, let G be an r-circumscribed $C_{40}H_{20}$ coronoid structure $K_2(3,1,2,r)$. Then,*

1. $W_e(G) = \frac{1}{10}(738r^5 + 5130r^4 + 13360r^3 + 17565r^2 + 10837r + 2520)$.

2. $W_{ve}(G) = \frac{1}{15}(1476r^5 + 11280r^4 + 32920r^3 + 48165r^2 + 33509r + 8820)$.

4.2 Carbon nanocones

Since the advent of carbon nanotubes and fullerenes, curved forms of carbon with conical tips consisting of curved graphite sheets with open cones are also known to exist and these structures have been of great interest for several researchers. These conical shaped nanocones are formed by removing a wedge and joining the edges to form the base of the conical part. Each edge of the polygonal cycle of dimension $m \geq 3$ on the base or the core forms a hexagon and hence surrounded by n layers of hexagons, as a consequence of which the outer boundary consists of $n+1$ hexagons, see Figure 7.

We now proceed to compute the edge-Wiener and vertex-edge-Wiener indices of carbon nanocones.

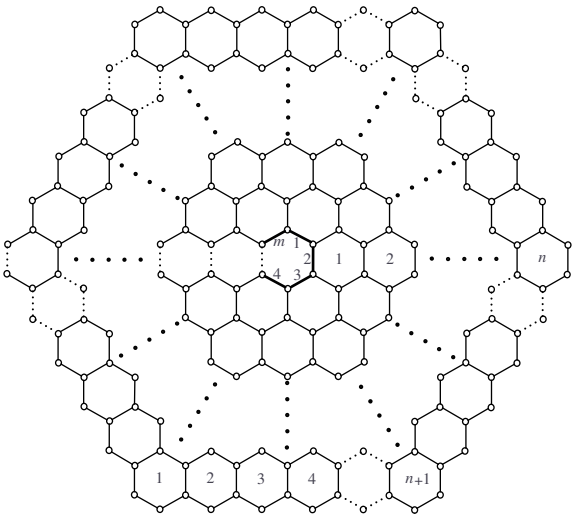

Figure 7: The structure of carbon nanocone $CNC_m(n)$.

Theorem 6. *Let G be the carbon nanocone structure $CNC_m(n)$. For m odd, $m > 3$ and $n \geq 1$,*

1. $W_e(G) = \frac{1}{160}(n+1)(45m^3n^3 + 480m^2n^4 + 45m^3n^2 + 800m^2n^3 - 912mn^4 + 20m^3n + 380m^2n^2 - 1313mn^3 + 20m^3 - 20m^2n - 377mn^2 - 80m^2 + 92mn + 60n^2 + 60m + 60n)$.

2. $W_{ve}(G) = \frac{1}{120}(n+1)(45m^3n^3 + 480m^2n^4 + 90m^3n^2 - 912mn^4 + 1090m^2n^3 + 45m^3n + 780m^2n^2 - 1693mn^3 + 200m^2n - 882mn^2 + 30m^2 - 173mn + 30n^2 - 60m + 60n + 30)$.

Proof. We know that $|V(G)| = m(n+1)^2$ and $|E(G)| = m(n+1)(3n+2)/2$. The Θ^*-classes along the periphery are formed by the linear hexagonal chain $\{E_{1i} : 1 \leq i \leq n\}$, and for each i, $E_{2i}, E_{3i}, \ldots, E_{mi}$ cuts are symmetric to E_{1i} with a total of mn cuts along the periphery. The graph with edge cut $G - E_{1i}$, and the quotient graph G/E_{1i} are shown in Figures 8(a) and 8(b), respectively. The strength-weighted values of the quotient graph G/E_{1i} are given below.

$a_1 = i(i+2n+2)$, $b_1 = \frac{1}{2}(3i - 2n + 6in + 3i^2 - 2)$,

$a_2 = |V(G)| - a_1$, $b_2 = |E(G)| - b_1 - (n+1+i)$,

$e_1 = (n+1+i)$.

We denote

$$W_e(G_1) = \sum_{i=1}^{n} W_e(G/E_i, (w_v^i, s_v^i), s_e^i) = \sum_{i=1}^{n} b_1 b_2,$$

$$W_{ve}(G_1) = \sum_{i=1}^{n} W_{ve}(G/E_i, (w_v^i, s_v^i), s_e^i) = \sum_{i=1}^{n} \big(a_1 b_2 + a_2 b_1\big).$$

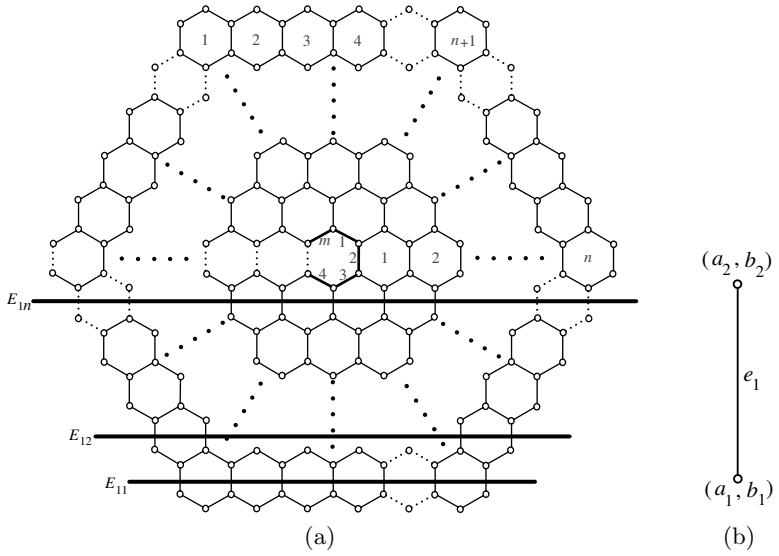

Figure 8: (a) $\{E_{1i} : 1 \leq i \leq n\}$ (b) Quotient graph G/E_{1i}.

Since m is odd, there exists a unique edge cut E_1 along the core. The graph with the edge cut E_1 along with its corresponding strength-weighted graph is depicted in Figures 9(a) and 9(b). The vertex strength-weight and edge-strength values are:

$a_3 = (n+1)^2$, $b_3 = \frac{3}{2}n(n+1)$, $e_2 = (n+1)$.

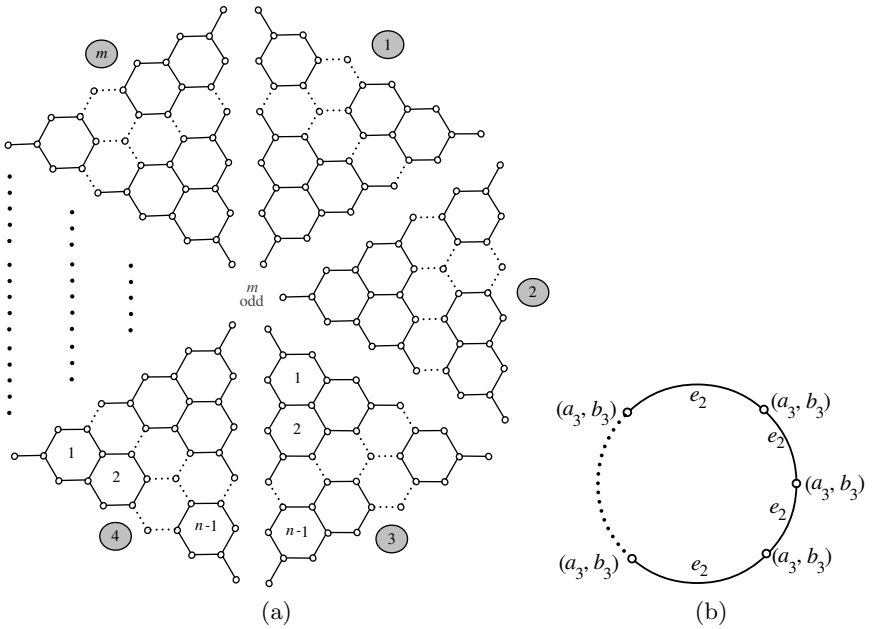

Figure 9: (a) $G - E_1$ (b) Quotient graph G/E_1.

We denote

$$W_e(G_2) = W_e(G/E_2, (w_v^1, s_v^1), s_e^1) = \ m \sum_{i=1}^{\frac{m-1}{2}} i b_3^2 + m \sum_{i=1}^{\frac{m-3}{2}} i e_2^2 + \frac{1}{4}(m-1)^2 b_3 e_2,$$

$$W_{ve}(G_2) = W_{ve}(G/E_2, (w_v^1, s_v^1), s_e^1) = \ 2m \sum_{i=1}^{\frac{m-1}{2}} i a_3 b_3 + \frac{1}{4}(m-1)^2 a_3 e_2.$$

Therefore, $W_e(G) = mW_e(G_1) + W_e(G_2)$ and $W_{ve}(G) = mW_{ve}(G_1) + W_{ve}(G_2)$, from which the formulae are deduced. □

Theorem 7. *Let G be the carbon nanocone structure $CNC_m(n)$. For m even, $m > 4$ and $n \geq 1$,*

1. $W_e(G) = \frac{1}{160} m(n+1)(45m^2n^3 + 480mn^4 + 105m^2n^2 + 800mn^3 - 912n^4 + 80m^2n + 200mn^2 - 1268n^3 + 20m^2 - 200mn - 212n^2 - 80m + 232n + 80)$.

2. $W_{ve}(G) = \frac{1}{120} m(n+1)(45m^2n^3 + 480mn^4 + 120m^2n^2 + 1090mn^3 - 912n^4 + 105m^2n + 690mn^2 - 1648n^3 + 30m^2 + 20mn - 732n^2 - 60m - 8n)$.

Proof. When m is even, the Θ^*-classes along the periphery are the same as defined in Theorem 6 and we proceed with the same computation for the peripheral cuts. For the core, the Θ^*-classes formed by $\{E_i : 1 \leq i \leq \frac{m}{2}\}$ are shown in Figure 10(a). The quotient graph G/E_i is the complete

graph K_2 and the vertex-weight and edge-strength values labeled on the Figure 10(b) are defined as follows: $a_4 = \frac{1}{2}m(n+1)^2$, $b_4 = \frac{1}{4}(n+1)(2m+3mn-4)$, and $e_3 = 2(n+1)$.

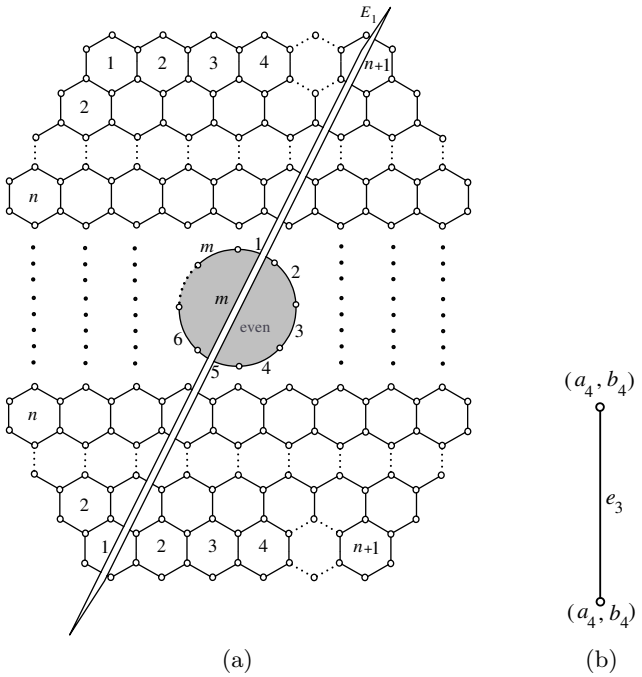

Figure 10: (a) $\{G - E_i : 1 \leq i \leq \frac{m}{2}\}$ (b) Quotient graph G/E_i.

Denote,

$W_e(G_3) = W_e(G/E_i, (w_v^i, s_v^i), s_e^i) = \ b_4^2,$

$W_{ve}(G_3) = W_{ve}(G/E_i, (w_v^i, s_v^i), s_e^i) = \ 2a_4b_4.$

Therefore, $W_e(G) = mW_e(G_1) + \frac{m}{2}W_e(G_3)$ and $W_{ve}(G) = mW_{ve}(G_1) + \frac{m}{2}W_{ve}(G_3)$, from which the formulae are obtained. □

4.3 SiO_2 nanotubes

SiO_2 nanotubes are among the most frequently utilized inorganic material as they possess unique physico-chemical properties. The mesoporous silica with empty channels lends to functionalization and attracts wide applications in drug discovery for controlled release and drug/gene delivery. It is formed by merging the pendant edges along the right and left sides of the octagonal mesh of an SiO_2 nanosheet of dimension $(p, q-1)$ to form a tubular structure with length p and circumeference q. The structure of SiO_2 nanotube with p rows and q columns shown in the Figure 11 clearly has

$|V(G)| = q(3p+4)$ vertices and $|E(G)| = 4q(p+1)$ edges [3].

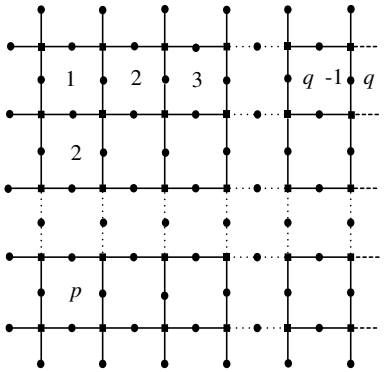

Figure 11: SiO_2 nanotube (p, q).

Theorem 8. *If G is the SiO_2 nanotube of dimension (p, q), where $p \geq 1$ and $q \geq 3$ is odd, then*

1. $W_e(G) = \frac{1}{3}q(16p^3q + 12p^2q^2 + 24p^2q + 3p^2 + 24pq^2 - pq + 12q^2 - 12q)$.

2. $W_{ve}(G) = q(p+1)(8p^2q + 6pq^2 + 14pq + p + 8q^2 + 4q - 4)$.

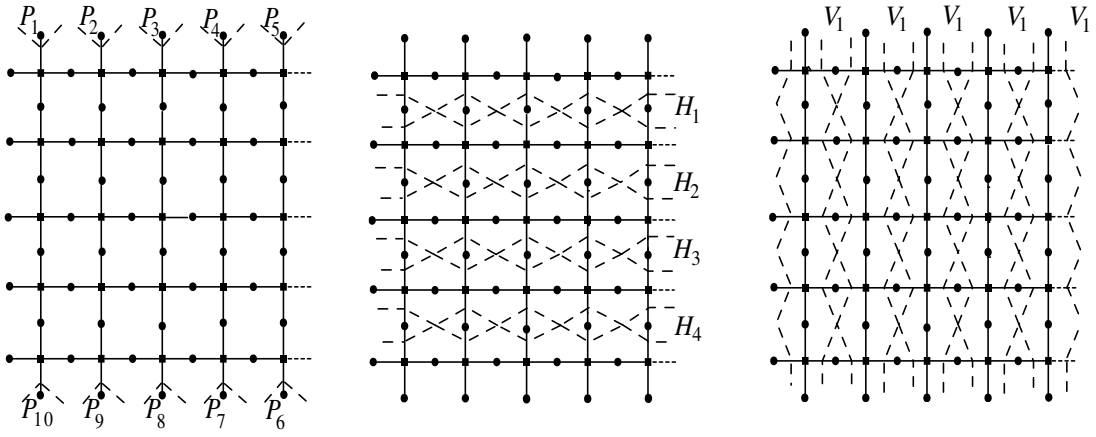

(a) (b) (c)

Figure 12: Convex cuts on G (a) P_i (b) H_i (c) V_1.

Proof. The Djokovič-Winkler relation when applied to the SiO_2 nanotube forms Θ^*-classes of G which are depicted in Figure 12. Each pendant edge cut forms its own Θ^*-class along the upper and lower open ends of G denoted as P_i, $\{P_i : 1 \leq i \leq 2q\}$, while the horizontal cuts denoted as H_i, $\{H_i : \ 1 \leq i \leq p\}$ are in the form of circular rings of G running along the p rows. When the length of the circular ring q is odd, there exists a unique vertical cut denoted as V_1. Clearly, the number of Θ^*-classes formed by G when q is odd is $2q + p + 1$. The corresponding quotient graphs of each cut

are shown in Figure 13 with the edge-strength value 1 on each edge. The vertex-strength-weighted values which are not given in the figure are presented in Table 3.

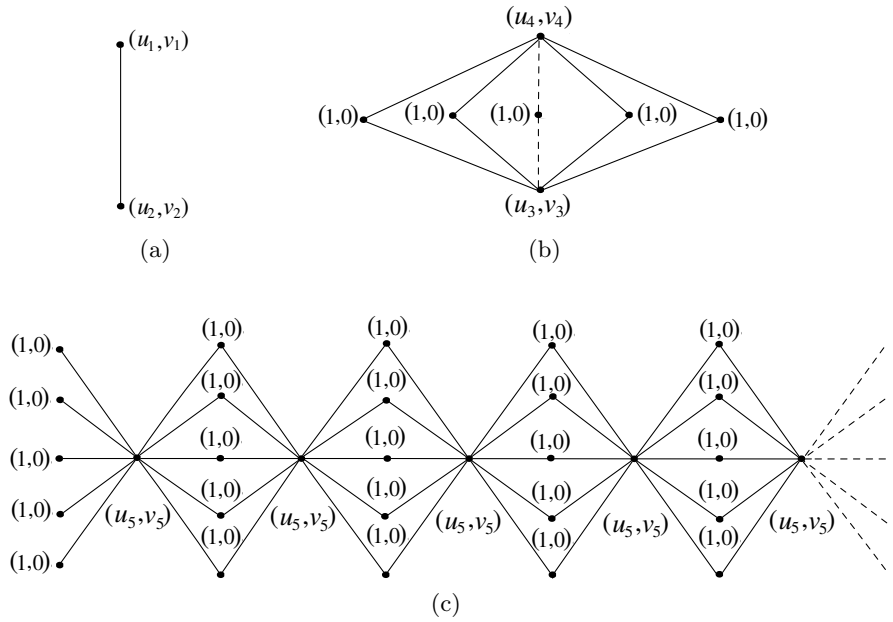

Figure 13: Quotient graphs (a) G/P_i (b) G/H_i (c) G/V_1.

Denote,

$$W_e(G_1) = W_e(G/P_i, (w_v^i, s_v^i), s_e^i) \;=\; 0,$$

$$W_{ve}(G_1) = W_e(G/P_i, (w_v^i, s_v^i), s_e^i) \;=\; u_1v_2,$$

$$W_e(G_2) = W_e(G/H_i, (w_v^i, s_v^i), s_e^i) \;=\; 2v_3v_4 + q(v_3+v_4) + q(q-1),$$

$$W_{ve}(G_2) = W_{ve}(G/H_i, (w_v^i, s_v^i), s_e^i) \;=\; 2(u_3v_4+v_3u_4) + q(u_3+u_4+v_3+v_4) + 2q(q-1),$$

$$\begin{aligned} W_e(G_3) &= W_e(G/V_1, (w_v^1, s_v^1), s_e^1) \\ &= q\Bigg(2\sum_{i=1}^{\frac{q-1}{2}} v_5^2 i + 2\sum_{i=1}^{q-1} v_5(p+1)i + 2\sum_{i=1}^{q-2}(p+1)^2 i + (q-1)(p+1)^2 + p(p+1)\Bigg), \end{aligned}$$

$$\begin{aligned} W_{ve}(G_3) &= W_{ve}(G/V_1, (w_v^1, s_v^1), s_e^1) \\ &= q\Bigg(4\sum_{i=1}^{\frac{q-1}{2}} u_5v_5 i + 2\sum_{i=1}^{\frac{q-1}{2}} v_5(p+1)(2i-1) + v_5q(p+1) + 2\sum_{i=1}^{q-1} u_5(p+1)i + 2\sum_{i=1}^{q-1}(p+1)^2 i \\ &\quad + 2p(p+1)\Bigg). \end{aligned}$$

Therefore, $W_e(G) = 2qW_e(G_1) + \sum_{i=1}^{p} W_e(G_2) + W_e(G_3)$ and $W_{ve}(G) = 2qW_{ve}(G_1) + \sum_{i=1}^{p} W_{ve}(G_2) +$

$W_{ve}(G_3)$, which yield the stated expressions.

Table 3: Strength-weighted values for the quotient graphs of SiO_2.

Quotient graphs	$\boldsymbol{w_v}$	$\boldsymbol{s_v}$
G/P_i;	$u_1 = 1$	$v_1 = 0$
$1 \leq i \leq 2q$	$u_2 = \lvert V(G)\rvert - 1$	$v_2 = \lvert E(G)\rvert - 1$
G/H_i;	$u_3 = 3qi$	$v_3 = q(4i-1)$
$1 \leq i \leq p$	$u_4 = 3q(p+1-i)$	$v_4 = q(4p-4i+3)$
G/V_1	$u_5 = 2p+3$	$v_5 = 2p+2$

□

Theorem 9. *If G is the SiO_2 nanotube of dimension (p,q), where $p \geq 1$ and $q \geq 2$ is even, then*

1. $W_e(G) = \frac{1}{3}q(16p^3q + 12p^2q^2 + 24p^2q + 6p^2 + 24pq^2 - pq + 6p + 12q^2 - 12q + 3)$.
2. $W_{ve}(G) = 2q(p+1)(4p^2q + 3pq^2 + 7pq + p + 4q^2 + 2q - 1)$.

Proof. The pendant and horizontal edge cuts follow the same computation as in Theorem 8. If the circular rings of SiO_2 nanotube are of even length, then there are $\frac{q}{2}$ vertical cuts denoted as $\{V_i : 1 \leq i \leq \frac{q}{2}\}$, see Figure 14(a), and thus the number of Θ^*-classes formed by G are $\frac{5}{2}q + p$. The vertex-strength-weighted values not given in the quotient graph depicted in the Figure 14(b) are $u_6 = \frac{3pq}{2} + 2q - (p+1)$, $v_6 = 2(pq + q - p - 1)$ and the edge-strength value on each edge is 1.
Now denote,

$$\begin{aligned} W_e(G_4) &= W_e(G/V_i, (w_v^i, s_v^i), s_e^i) \\ &= 2(v_6^2 + 2v_6(p+1) + (p+1)^2 + p(p+1)), \\ W_{ve}(G_4) &= W_{ve}(G/V_i, (w_v^i, s_v^i), s_e^i) \\ &= 4(u_6v_6 + v_6(p+1) + u_6(p+1) + (p+1)^2 + p(p+1)). \end{aligned}$$

Therefore, $W_e(G) = 2qW_e(G_1) + \sum_{i=1}^{p} W_e(G_2) + \frac{q}{2}W_e(G_4)$ and $W_{ve}(G) = 2qW_{ve}(G_1) + \sum_{i=1}^{p} W_{ve}(G_2) + \frac{q}{2}W_{ve}(G_4)$, from which the formulae are deduced.

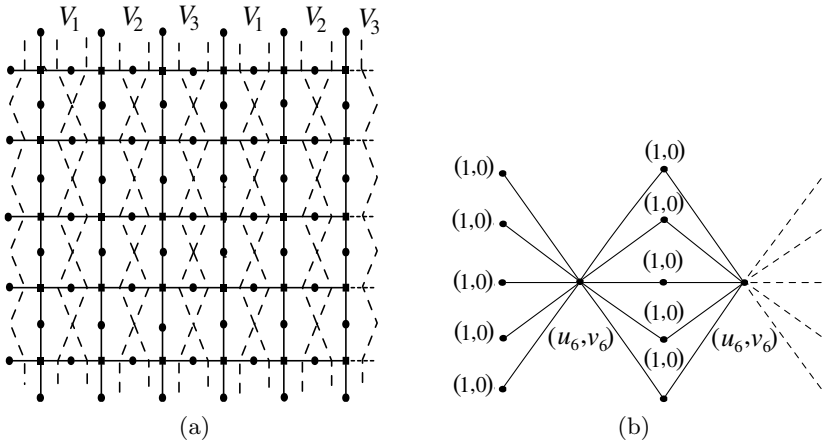

Figure 14: (a) Convex cut V_i (b) Quotient graph G/V_i.

□

5 W_e and W_{ve} of subdivisions of partial cubes

We begin this section by recalling the PI index and the standard cut-method for W_e, W_{ve} and PI indices. The PI index of a simple graph G is defined as

$$PI(G) \quad = \sum_{e=uv \in E(G)} \Big[m_u(e|G) + m_v(e|G) \Big],$$

where m_u is the number of edges lying closer to u than to v, and m_v is defined analogously. If G is a partial cube and $\mathcal{F}(G) = \{F_1, \ldots, F_k\}$ its Θ-partition, then recall that $G - F_i$ consists of two connected components. If $n_1(F_i)$ and $n_2(F_i)$ denote the order, and $m_1(F_i)$ and $m_2(F_i)$ the size of these components, then

- [35] $W_e(G) = \sum_{i=1}^{k} m_1(F_i)\ m_2(F_i)$,
- [1] $W_{ve}(G) = \sum_{i=1}^{k} [n_1(F_i)\ m_2(F_i) + n_2(F_i)\ m_1(F_i)]$,
- [18] $PI(G) = |E(G)|^2 - \sum_{i=1}^{k} |F_i|^2$.

The subdivision $Sub(G)$ of a graph G is obtained by replacing every edge uv of G by a vertex x_{uv} and connecting x_{uv} with u and v. The number of vertices and edges of $Sub(G)$ are $|V(G)| + |E(G)|$ and $2|E(G)|$, respectively. Let G be a partial cube with Θ-classes $F_i = \{u_j v_j : 1 \leq j \leq s\}$. It has been proved in [3] that if $|F_i| \geq 3$, then the quotient graph is K_2 with vertex-strength-weighted

values $(n_1(F_i), m_1(F_i))$ and $(n_2(F_i), m_2(F_i))$ and edge-strength value $|F_i|$ as shown in the Figure 15(a). The Θ^*-classes of $Sub(G)$ are then $F_i' = \{u_jx_j, x_jv_j : 1 \leq j \leq s\}$, the corresponding quotient graph being the complete bipartite graph $K_{2,|F_i|}$ with edge-strength 1 for all the edges and vertex-strength-weighted values for one partite vertices as $(a_i(F_i'), b_i(F_i'))$ and $(c_i(F_i'), d_i(F_i'))$ and the other partite vertices $(1, 0)$ each as shown in the Figure 15(b) where $a_i(F_i') = n_1(F_i) + m_1(F_i)$, $b_i(F_i') = 2m_1(F_i)$, $c_i(F_i') = n_2(F_i) + m_2(F_i)$, and $d_i(F_i') = 2m_2(F_i)$. If $|F_i| \leq 2$ (that is, if $s = 1$ or 2), then we have $F_i' = \{u_jx_j, x_jv_j : 1 \leq j \leq s\}$ which is a union of two Θ^*-classes in $Sub(G)$ and the above arguments hold.

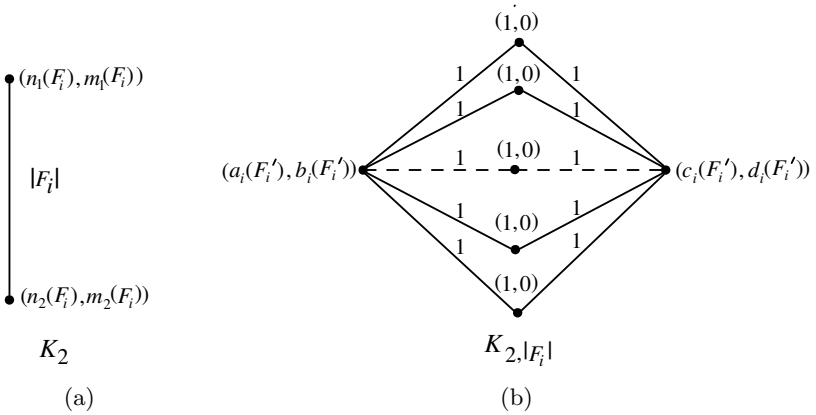

Figure 15: Quotient graphs (a) G/F_i (b) $Sub(G)/F_i'$.

Theorem 10. *Let $\mathcal{F}(G) = \{F_1, \ldots, F_k\}$ be the Θ-partition of a partial cube G and let $\mathcal{F}'\big(Sub(G)\big) = \{F_1', \ldots, F_k'\}$ be the Θ^*-partition of $Sub(G)$. If $TI \in \{W_e, W_{ve}\}$, then*

$$TI\big(Sub(G)\big) = \sum_{i=1}^{k} TI\big(K_{2,|F_i|}, (w_v^i, s_v^i), s_e^i\big)\,.$$

Furthermore,

1. $W_e\big(Sub(G)\big) = 8W_e(G) + PI(G) + |E(G)|(|E(G)| - 1)$.

2. $W_{ve}\big(Sub(G)\big) = 4W_{ve}(G) + 8W_e(G) + PI(G) + |E(G)|(2|E(G)| + |V(G)| - 2)$.

Proof. By Theorem 3, it is easy to see that $TI\big(Sub(G)\big) = \sum_{i=1}^{k} TI\big(Sub(G)/F_i, (w_v^i, s_v^i), s_e^i\big)$. As noted above, the quotient graph $Sub(G)/F_i$ is isomorphic to $K_{2,|F_i|}$ with strengths and weights as given in Figure 15. Therefore, $TI\big(Sub(G)\big) = \sum_{i=1}^{k} TI\big(K_{2,|F_i|}, (w_v^i, s_v^i), s_e^i\big)$. Applying the concept of

strength-weighted functions of quotient graphs, we compute the indices as follows.

$$
\begin{aligned}
(i)\ W_e(Sub(G)) &= \sum_{i=1}^{k} W_e\big(K_{2,|F_i|}, (w_v^i, s_v^i), s_e^i\big) \\
&= \sum_{i=1}^{k} \Big[2b_i(F_i')d_i(F_i') + |F_i|\big[b_i(F_i') + d_i(F_i')\big] + |F_i|(|F_i|-1) \Big] \\
&= \sum_{i=1}^{k} \Big[2(2m_1(F_i))(2m_2(F_i)) + |F_i|\big[2m_1(F_i) + 2m_2(F_i) + |F_i| - 1\big] \Big] \\
&= 8W_e(G) + PI(G) + |E(G)|(|E(G)|-1). \\
(ii)\ W_{ve}(Sub(G)) &= \sum_{i=1}^{k} W_{ve}\big(K_{2,|F_i|}, (w_v^i, s_v^i), s_e^i\big) \\
&= \sum_{i=1}^{k} \Big[2\big[a_i(F_i')d_i(F_i') + b_i(F_i')c_i(F_i')\big] + |F_i|\big[b_i(F_i') + d_i(F_i') + a_i(F_i') + c_i(F_i')\big] \\
&\quad + 2|F_i|(|F_i|-1) \Big] \\
&= \sum_{i=1}^{k} \Big[2\big[(n_1(F_i) + m_1(F_i))2m_2(F_i) + (n_2(F_i) + m_2(F_i))(2m_1(F_i))\big] \\
&\quad + |F_i|\big[3m_1(F_i) + 3m_2(F_i) + n_1(F_i) + n_2(F_i) + 2|F_i| - 2\big] \Big] \\
&= 4W_{ve}(G) + 8W_e(G) + PI(G) + |E(G)|(2|E(G)| + |V(G)| - 2).
\end{aligned}
$$

□

The results obtained in Subsection 4.3 can also be obtained alternatively from Theorem 10 by considering SiO_2 nanotube as the subdivision of $P_n \,\square\, C_m$, provided that the indices W_e, W_{ve}, and PI are known for $P_n \,\square\, C_m$. Moreover, Theorem 10 can be readily applied to SiO_2 nanotorus as the subdivision of $C_n \,\square\, C_m$. We now demonstrate the Theorem 10 on the subdivision of circumcoronene series to compute their W_e and W_{ve} indices. The structure of circumcornene series H_n is depicted in Figure 16.

Theorem 11. *For a circumcoronene series of benzenoid system H_n, $n \geq 1$,*

1. [35] $W_e(H_n) = \frac{3}{10}(246n^5 - 340n^4 + 140n^3 - 5n^2 - n)$.
2. [1] $W_{ve}(H_n) = \frac{1}{5}(492n^5 - 340n^4 + 25n^2 + 3n)$.
3. [1] $PI(H_n) = 81n^4 - 68n^3 + 12n^2 - n$.

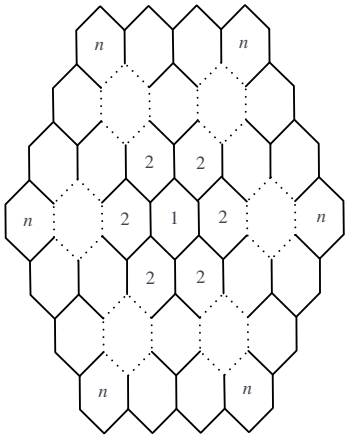

Figure 16: The structure of circumcoronene H_n.

Combining Theorems 10 and 11, we obtain the following theorem.

Theorem 12. *If $n \geq 1$, then*

1. $W_e(Sub(H_n)) = \frac{1}{5}n(2952n^4 - 3495n^3 + 1340n^2 - 30n - 17)$.

2. $W_{ve}(Sub(H_n)) = n(984n^4 - 899n^3 + 268n^2 + 8n - 1)$.

6 Conclusion

This study involves the investigation of edge and vertex-edge variants of Wiener indices, in the main part of the paper for strength-weighted graphs, and in the last part for subdivisions of partial cubes. The principle key idea involved is the dissection of a graph with respect to the edges using the transitive closure property of Djoković-Winkler relation. We have applied the obtained results of the variants under study for strength-weighted graphs on the molecular graphs of coronoid systems, carbon nanocones and SiO_2 nanostructures. Further, the implementation on the subdivision of a family of partial cubes has been carried over on the circumcoronene series. We anticipate that the newly developed techniques will have several chemical applications in computer assisted drug discovery and predictive computational toxicology.

Acknowledgements

S. K. acknowledges the financial support from the Slovenian Research Agency (research core funding No. P1-0297 and projects J1-9109, N1-0095, N1-0108).

References

[1] M. Arockiaraj, J. Clement, K. Balasubramanian, Analytical expressions for topological properties of polycyclic benzenoid networks, J. Chemometr. **30**(11) (2016) 682–697.

[2] M. Arockiaraj, J. Clement, K. Balasubramanian, Topological indices and their applications to circumcised donut benzenoid systems, kekulenes and drugs, Polycycl. Aromat. Comp. DOI: 10.1080/10406638.2017.1411958.

[3] M. Arockiaraj, S. Klavžar, S. Mushtaq, K. Balasubramanian, Distance-based topological indices of SiO_2 nanosheets, nanotubes and nanotori, J. Math. Chem. **57**(1) (2019) 343-369.

[4] M. Arockiaraj, A.J. Shalini, Extended cut method for edge Wiener, Schultz and Gutman indices with applications, MATCH Commun. Math. Comput. Chem. **76**(1) (2016) 233–250.

[5] K. Balasubramanian, Mathematical and computational techniques for drug discovery: promises and developments, Curr. Top. Med. Chem. DOI: 10.2174/1568026619666190208164005.

[6] K. Balasubramanian, S.P. Gupta, Quantum molecular dynamics, topological, group theoretical, and graph theoretical studies of protein-protein interactions, Curr. Top. Med. Chem. DOI:10.2174/1568026619666190304152704.

[7] A. Chen, X. Xiong, F. Lin, Explicit relation between the Wiener index and the edge-Wiener index of the catacondensed hexagonal systems, Appl. Math. Comput. **273** (2016) 1100–1106

[8] M. Črepnjak, N. Tratnik, The Szeged index and the Wiener index of partial cubes with applications to chemical graphs, Appl. Math. Comput. **309** (2017) 324–333.

[9] M. Črepnjak, N. Tratnik, The edge-Wiener index, the Szeged indices and the PI index of benzenoid systems in sub-linear time, MATCH Commun. Math. Comput. Chem. **78**(3) (2017) 675–688.

[10] P. Dankelmann, I. Gutman, S. Mukwembi, H.C. Swart, The edge-Wiener index of a graph, Discrete Math. **309**(10) (2009) 3452–3457.

[11] D. Djoković, Distance preserving subgraphs of hypercubes, J. Combin. Theory Ser. B **14**(3) (1973) 263–267.

[12] A.A. Dobrynin, Distance of iterated line graphs, Graph Theory Notes N. Y. **37** (1999) 8–9.

[13] I. Gutman, Distance of line graphs, Graph Theory Notes N. Y. **31** (1996) 49–52.

[14] A. Iranmanesh, M. Azari, Edge-Wiener descriptors in chemical graph theory: a survey, Curr. Org. Chem. **19**(3) (2015) 219–239.

[15] A. Iranmanesh, I. Gutman, O. Khormali, A. Mahmiani, The edge versions of the Wiener index, MATCH Commun. Math. Comput. Chem. **61**(3) (2009) 663–672.

[16] O. Ivanciuc, QSAR comparative study of Wiener descriptors for weighted molecular graphs, J. Chem. Inf. Comput. Sci. **40**(6) (2000) 1412–1422.

[17] O. Ivanciuc, T. Ivanciuc, D. Cabrol-Bass, A.T. Balaban, Comparison of weighting schemes for molecular graph descriptors: Application in quantitative structure-retention relationship models for alkylphenols in gas-liquid chromatography, J. Chem. Inf. Comput. Sci. **40**(3) (2000) 732–743.

[18] P.E. John, P.V. Khadikar, J. Singh, A method of computing the PI index of benzenoid hydrocarbons using orthogonal cuts, J. Math. Chem. **42**(1) (2007) 37–45.

[19] A. Kelenc, S. Klavžar, N. Tratnik, The edge-Wiener index of benzenoid systems in linear time, MATCH Commun. Math. Comput. Chem. **74**(3) (2015) 521–532.

[20] M.H. Khalifeh, H. Yousefi-Azari, A.R. Ashrafi, S.G. Wagner, Some new results on distance-based graph invariants, Eur. J. Comb. **30**(5) (2009) 1149–1163.

[21] S. Klavžar, On the canonical metric representation, average distance, and partial Hamming graphs, Eur. J. Combin. **27**(1) (2006) 68–73.

[22] S. Klavžar, I. Gutman, Wiener number of vertex-weighted graphs and a chemical application, Discrete Appl. Math. **80**(1) (1997) 73–81.

[23] S. Klavžar, I. Gutman, B. Mohar, Labeling of benzenoid systems which reflects the vertex-distance relation, J. Chem. Inf. Comput. Sci. **35**(3) (1995) 590–593.

[24] S. Klavžar, M.J. Nadjafi-Arani, Wiener index in weighted graphs via unification of Θ^*-classes, Eur. J. Combin. **36** (2014) 71–76.

[25] S. Klavžar, M.J. Nadjafi–Arani, Cut method: update on recent developments and equivalence of independent approaches, Curr. Org. Chem. **19**(4) (2015) 348–358.

[26] M. Knor, P. Potočnik, R. Škrekovski, Relationship between the edge-Wiener index and the Gutman index of a graph, Discrete Appl. Math. **167** (2014) 197–201.

[27] M. Knor, R. Škrekovski, A. Tepeh, An inequality between the edge-Wiener index and the Wiener index of a graph, Appl. Math. Comput. **269** (2015) 714–721.

[28] M. Knor, R. Škrekovski, A. Tepeh, Mathematical aspects of Wiener index, Ars Math. Contemp. **11**(2) (2016) 327–352.

[29] S. Nandi, M.C. Bagchi, QSAR of aminopyrido[2,3-d]pyrimidin-7-yl derivatives: Anticancer drug design by computed descriptors, J. Enzyme Inhib. Med. Chem. **24**(4) (2009) 937–948.

[30] A. Soltani, A. Iranmanesh, Z.A. Majid, The multiplicative version of the edge-Wiener index, MATCH Commun. Math. Comput. Chem. **71**(2) (2014) 407–416.

[31] A. Thakur, M. Thakur, N. Kakani, A. Joshi, S. Thakur, A. Gupta, Application of topological and physicochemical descriptors: QSAR study of phenylamino-acridine derivatives, ARKIVOC **2004**(14) (2004) 36–43.

[32] N. Tratnik, Generalized cut method for computing the edge-Wiener index, arXiv:1902.03153 [math.CO] 8 Feb 2019.

[33] H. Wiener, Structural determination of paraffin boiling points, J. Am. Chem. Soc. **69**(1) (1947) 17–20.

[34] P. Winkler, Isometric embeddings in products of complete graphs, Discrete Appl. Math. **7**(2) (1984) 221–225.

[35] H. Yousefi-Azari, M.H. Khalifeh, A.R. Ashrafi, Calculating the edge-Wiener and Szeged indices of graphs, J. Comput. Appl. Math. **235**(16) (2011) 4866–4870.

[36] X.B. Zhou, W.J. Han, J. Chen, X.Q. Lu, QSAR study on the interactions between antibiotic compounds and DNA by a hybrid genetic-based support vector machine, Monatsh. Chem. **142**(9) (2011) 949–959.

[37] P. Žigert Pleteršek, The edge-Wiener index and the edge-hyper-Wiener index of phenylenes, Discrete Appl. Math. **255**(1)(2019) 326–333.